

# Orthorhombic crystalline field splitting on orbital and magnetic orders in $\text{KCuF}_3$

Dong-Meng Chen<sup>1,2</sup> and Liang-Jian Zou<sup>1</sup>

<sup>1</sup> Key Laboratory of Materials Physics, Institute of Solid State Physics,  
Chinese Academy of Sciences, P. O. Box 1129, Hefei 230031, China and

<sup>2</sup> Graduate School of the Chinese Academy of Sciences

(Dated: December 5, 2018)

Magnetic and orbital structures in  $\text{KCuF}_3$  are revisited by the cluster self-consistent field approach developed recently. We clearly showed that due to the inherent frustration, the ground state of the system with the superexchange and Jahn-Teller phonon-mediated orbital couplings is highly degenerate without broken symmetry; the orthorhombic crystalline field splitting arising from static Jahn-Teller distortion stabilizes the orbital ordering, about 42% in the  $x^2 - y^2$  orbit and 58% in the  $3z^2 - r^2$  orbit in sublattices. The magnetic moment of Cu is considerably reduced to  $0.49\mu_B$ , and the magnetic coupling strengths are highly anisotropic,  $J_c/J_{ab} \approx 26$ . These results are in agreement with the experiments, implying that as an orbital selector, the crystalline field plays an essential role in stabilizing the ground state of  $\text{KCuF}_3$ . The 1s-3d resonant X-ray scattering amplitudes in  $\text{KCuF}_3$  with the *type-a* and *type-d* structures are also presented.

PACS numbers: 71.27.+a, 75.25.+z, 71.70.Ch, 71.70.Ej

## I. INTRODUCTION

Three-dimensional pseudocubic perovskite  $\text{KCuF}_3$  has attracted extensive interest since 1970s for its unusual low-dimensional antiferromagnetic (AFM) and orbital ground state. In this compound the  $\text{Cu}^{2+}$  ion has  $3d^9$  configuration with the fulfilled  $t_{2g}$  orbitals and the twofold-degenerate  $e_g$  orbitals occupied by one hole, the latter leads to the Jahn-Teller (JT) effect. The orbital degree of freedom of the holes interplays with spin and lattice degrees of freedom, which results in the orbital regular occupation in real space, i.e. the orbital ordering. The orbital polarization of the hole is usually depicted by a pseudospin operator,  $\vec{\tau} = 1/2 \sum_{ab} c_a^\dagger \sigma_{ab} c_b$ , here  $c_a^\dagger$  creates a hole at orbit  $a$ , and  $\sigma$  denotes the Pauli matrix.  $\tau_i^z = 1/2$  represents the full orbital polarization in  $|3z^2 - r^2\rangle$  and  $\tau_i^z = -1/2$  the orbital polarization in  $|x^2 - y^2\rangle$ . The orbital polarization degree represented by  $\langle \tau_i \rangle$  is called the *orbitalization*. Up to date, the orbital ordering is considered as the essential factor in stabilizing the abnormal magnetic structure in  $\text{KCuF}_3$ , and is observed recently by the resonant x-ray scattering (RXS) experiment<sup>1,2</sup>. Though it has been known very early that the combination of the electronic superexchange (SE) interaction and the JT effect is responsible for the orbital ordering in  $\text{KCuF}_3$ <sup>3</sup>, as shown in the following, the uniqueness of the orbital ground state and the magnetic and the orbital experimental results available are not well understood theoretically<sup>3,4,5,6,7,8</sup>.

In pseudocubic perovskite  $\text{KCuF}_3$  the adjacent  $\text{CuF}_6$  octahedra in (**a,b**) plane are elongated along the **a** and **b** axis alternatively due to the JT distortion. There are two tetragonal crystal polytypes discriminated as *type-a* by the antiferro-distortion stacking the **ab**-planes and *type-d* by the ferro-distortion stacking the **ab**-planes<sup>9,10</sup>. The RXS results<sup>1,2</sup> showed that in  $\text{KCuF}_3$  the ground state is the G-type antiferro-orbital (AFO) order for *type-a* structure; and the C-type AFO arrangement for *type-d*

structure. In these two structures the Cu spins are A-type AFM order below 39 K for *type-a* and below 22K for *type-d*; in both situations the averaged magnetic moment of each Cu ion is about  $0.49 \mu_B$  at 4 K<sup>11</sup>. The magnetic couplings in  $\text{KCuF}_3$  are highly anisotropic, and the neutron scattering experiment<sup>11,23</sup> gave rise to  $J_{ab}/J_c \sim -0.01$ , suggesting significant one-dimensional character.

More than thirty years ago Kugel and Khomskii<sup>3</sup> proposed a SE model from the pure electron-electron interaction, the so-called *K-K model*, between Cu 3d electrons to describe the role of orbital degree of freedom in the A-type AFM structure; by comparing the energies of different magnetic structures in the classical approximation, they found the A-type AFM is stable; while for the orbital configuration, the G-AFO ordering is degenerate with the C-type AFO ordering. Further they showed<sup>19</sup> that the anharmonic distortion from the JT effect lowering the lattice symmetry might give rise to the orbital ordering. In fact the orbital part of the *K-K model* is inherently frustrated<sup>12</sup>; Feiner *et al.*<sup>13,14</sup> pointed out that due to quantum spin-orbital wave excitations, this frustrated SE interaction leads to a spin-orbital liquid state; and when a tetragonal crystalline field (CF) splitting,  $E_z$ , is applied to the K-K model, the ground state is ferro-orbital at large  $E_z$ . Some other authors<sup>7</sup> emphasized that the phonon-mediated orbital coupling arising from the cooperative JT effect gives rise to the orbital ordering. However, Khomskii and Mostovoy<sup>12</sup> recently pointed out that this effective orbital-orbital interaction is also inherently frustrated, similar to the orbital part in the electronic SE interaction. In this case the JT orbital interaction combining the SE interaction favors the para-orbital or orbital liquid phase since the quantum fluctuations of the pseudospins  $\vec{\tau}$  are still very large.

Under the cooperative JT distortion, the low-temperature crystal structure of  $\text{KCuF}_3$  is tetragonal; meanwhile, the local crystalline field of  $\text{CuF}_6$  arising from the static Jahn-Teller distortion is orthorhombic.

The effect of the orthorhombic CF splitting on the orbital order and the magnetic order of  $\text{KCuF}_3$  was seldom taken into account in the past literatures. In the recent *ab initio* study within the LDA+U scheme, Binggeli and Altarelli<sup>17</sup> found that in the *type-a* JT distorted tetragonal structure, the orbital ordering is G-type AFO and the orbital RXS intensity agrees with the experimental observation; in contrast, Medvedeva *et al.*<sup>5</sup> found in the absence of the JT distortion, the C-type AFO ground state is degenerate with G-type AFO. Therefore the realistic orthorhombic CF splitting is crucial for the stable orbital-ordered ground state. Nevertheless, the *ab initio* study underestimates the spin and orbital quantum fluctuations in  $\text{KCuF}_3$ . It deserves to explore in detail on how the spin and orbital quantum fluctuations and the role of orthorhombic CF splitting on the orbital ordered ground state.

In this paper, after deriving the orthorhombic CF splitting, we study the combination effect of the electronic SE coupling, the effective orbital JT coupling and the CF splitting on the orbital and spin ground state. Utilizing the cluster self-consistent field (Cluster-SCF) approach<sup>20</sup>, we demonstrated that the orthorhombic CF splitting plays a key role in stabilizing the orbital ordered phases of  $\text{KCuF}_3$  in *type a* and *type d* structures: the orbital and spin fluctuations considerably reduce the magnetic moment of Cu spin to  $0.49\mu_B$ , and the strong anisotropy in spin correlation functions and orbital correlation functions results in the ratio of magnetic coupling strengths,  $J_c/J_{ab} \approx 26$ . The azimuthal dependence of the RXS intensity is also calculated for the  $1s - 3d$  excitation event. The experimental results could be consistently understood in the present theory. The rest of this paper is organized as follows: in Sec.II we describe the effective Hamiltonian and the Cluster-SCF method; then we present the theoretical results and discuss the role of CF in magnetic and orbital orderings in Sec.III; the azimuthal angle dependence of the RXS intensity is given in Sec.IV; and the last section is devoted to the remarks and summary.

## II. MODEL HAMILTONIAN AND CLUSTER-SCF METHOD

According to the preceding analysis, the effective Hamiltonian of  $\text{KCuF}_3$  contains three parts

$$H = H_{SE} + H_{JT} + H_{CF} \quad (1)$$

The first term  $H_{SE}$  represents the electronic SE coupling between two nearest-neighbor (N.N)  $e_g$  holes of  $\text{Cu}^{2+}$  ions derived from the generalized twofold degenerate Hubbard model<sup>18</sup>,

$$H_{SE} = \sum_{\substack{\langle ij \rangle_l \\ l=x,y,z}} (J_1 \vec{s}_i \cdot \vec{s}_{j_l} + J_2 I_i^l \vec{s}_i \cdot \vec{s}_{j_l} + J_3 I_i^l I_{j_l}^l \vec{s}_i \cdot \vec{s}_{j_l} + J_4 I_i^l I_{j_l}^l) \quad (2)$$

where the constants  $J_1$ ,  $J_2$ ,  $J_3$  and  $J_4$  are the superexchange coupling strengths:  $J_1 = 8t^2 [U/(U^2 - J_H^2) - J_H/(U_1^2 - J_H^2)]$ ,  $J_2 = 16t^2 [1/(U_1 + J_H) + 1/(U + J_H)]$ ,  $J_3 = 32t^2 [U_1/(U_1^2 - J_H^2) - J_H/(U^2 - J_H^2)]$ , and  $J_4 = 8t^2 [(U_1 + 2J_H)/(U_1^2 - J_H^2) + J_H/(U^2 - J_H^2)]$ , respectively.  $U$  and  $U_1$  are the intra- and inter-orbital Coulomb interactions, and  $J_H$  is the Hund's coupling. Due to the *pd* hybridization between Cu  $3d$  and F  $2p$  orbitals<sup>17</sup>, we take the relationship  $U = U_1 + J_H$ . The parameters  $U=7.5$  eV and  $J_H=0.9$  eV are adopted from the constrained LDA computation for  $\text{KCuF}_3$ <sup>4</sup>. The hopping integral along the  $c$  direction is the largest,  $t_{3z^2-r^2,3z^2-r^2} = 4t$ , we take  $t=0.12$  eV, thus the energy scale of the superexchange coupling is  $J = 16t^2/U = 30.7$  meV.  $\vec{s}_i$  denotes the spin at site  $i$ , while the operator  $I_i^l = \cos(2\pi m_l/3) \tau_i^z - \sin(2\pi m_l/3) \tau_i^x$ , the index  $l$  denotes the direction of a bond,  $l = x, y$  or  $z$ , corresponding to the crystal axes,  $a, b$  and  $c$ ;  $\langle ij \rangle_l$  connects site  $i$  and its nearest-neighbor site  $j$  along the  $l$  direction, and  $(m_x, m_y, m_z) = (1, 2, 3)$ . The orbital pseudospin operators  $\tau_i^z$  and  $\tau_i^x$  are the components of  $\vec{\tau}$ .

The second term in Eq.(1) represents the phonon-mediated orbital coupling from the cooperative JT effect. Through eliminating the phonon operator, one can get an effective orbital-orbital interaction  $H_{JT}$ <sup>7,12,19</sup>,

$$H_{JT} = g_{JT} \sum_{\substack{\langle ij \rangle_l \\ l=x,y,z}} I_i^l I_{j_l}^l \quad (3)$$

It has the same form as the orbital part of the last term in Eq.(2), both of them contribute to the orbital frustration and quantum fluctuations. The Jahn-Teller distortion energy  $E_{JT} \sim 130$  meV<sup>1</sup>,  $g_{JT}$  is the same order as  $E_{JT}$  in magnitude.

The static JT effect distorts the symmetry of  $\text{CuF}_6$  octahedra to orthorhombic, in which there are three different Cu-F bonds, the medium length Cu-F bond is along the  $z$ -axis, the long and short Cu-F bonds alternate along the  $x$  and the  $y$  axes. All of the F-Cu-F angles are  $90^\circ$  or  $180^\circ$ , and no rotation is found<sup>10</sup>. Employing the point charge model to calculate the CF splitting, we obtain the orthorhombic CF splitting of the holes,

$$H_{CF} = \sum_i (V_{iz} \tau_i^z + V_{ix} \tau_i^x) \quad (4)$$

The intermediate compression of the Cu-F bond along  $c$ -axis implies the sign of  $V_{iz}$  is negative for the hole,  $V_{iz} < 0$ , since the compressed octahedra lifts the  $|3z^2 - r^2\rangle$  orbit, thus the  $|3z^2 - r^2\rangle$  orbit is in favor of hole occupation; and the component  $V_{ix}$  mixes the two  $e_g$  orbitals at site  $i$ . The former favors of the orbital ordering, while the latter tends to destroy the orbital ordering. Using the crystal structure data in Ref.10 we estimate the ratio  $|V_x/V_z| \sim 2$ , and  $V_z$  is the same order in magnitude as the superexchange interaction.

It is a huge challenge to treat the spin-orbital correlations and fluctuations and to find the ground state of such

strongly correlated systems with high accuracy. To study the groundstate properties, we apply the Cluster-SCF approach<sup>20</sup> developed recently to deal with the complicated spin-orbital Hamiltonian (1). This approach combines the exact diagonalization for a central cluster and the self-consistent field for surrounding atoms. The main idea of the approach is described as follows: consider a proper cluster, usually the unit cell of the compounds, in which the 3d electrons interact via Eq.(1). First, we substitute the spin coupling  $\vec{s}_i \cdot \vec{s}_j$  in the cluster Hamiltonian,  $H$ , with the spin correlation functions  $\langle \vec{s}_i \cdot \vec{s}_j \rangle$ , here

$$H = \sum_{\substack{\langle ij \rangle_l \\ l=x,y,z}} [F(\vec{\tau}_i, \vec{\tau}_j) \vec{s}_i \cdot \vec{s}_{j_l} + (J_4 + g_{JT}) I_i^l I_{j_l}^l] + \sum_i (V_{iz} \tau_i^z + V_{ix} \tau_i^x), \quad (5)$$

with

$$F(\vec{\tau}_i, \vec{\tau}_j) = J_1 + \frac{J_2}{2} (I_i^l + I_{j_l}^l) + J_3 I_i^l I_{j_l}^l.$$

And then diagonalize the orbital part of the cluster Hamiltonian in the presence of the orbital SCF<sup>21</sup>, hence obtain the orbitalization  $\langle \vec{\tau} \rangle$  and the orbital correlation functions  $\langle \vec{\tau}_i \cdot \vec{\tau}_j \rangle$ . Second, substitute the orbital operator,  $\vec{\tau}$ , and their coupling  $\vec{\tau}_i \cdot \vec{\tau}_j$  with the orbitalization and the orbital correlation functions obtained, and diagonalize the spin part of the cluster Hamiltonian in the presence of the spin SCF, thus obtain a new set of spin correlation functions. Repeat the above steps iteratively until the groundstate energy, the spin and the orbital correlation functions self-consistently converge to the accuracies. The advantage of the present approach superior to the traditional mean-field method is that the short-range spin and orbital correlations and quantum fluctuations are taken into account. In comparison with the traditional mean-field method, one can obtain more better results for some simple models with large quantum fluctuations, such as the Heisenberg AFM model<sup>21</sup>.

### III. RESULTS AND DISCUSSIONS

In this section we first investigate the ground state of KCuF<sub>3</sub> under the electronic SE interaction and the JT phonon-mediated orbital interaction, then explore the role of orthorhombic CF splitting in the ground state.

#### A. Superexchange and JT Orbital Interactions

For the electronic SE coupling in Eq.(2), the mean-field results<sup>3,5</sup> suggested the staggered orbital order with  $x^2-z^2/y^2-z^2$  orbitals. However, utilizing the cluster-SCF approach, we find the spin-orbital ground state is composed of numerous degenerate states: such as the *Neel*

AFM order with ferro-orbital structure, in which the hole occupies one of the three orbitals among the  $|3x^2 - r^2\rangle$ , the  $|3y^2 - r^2\rangle$  and the  $|3z^2 - r^2\rangle$  orbitals; or the *Neel* AFM order with the alternating plaquette valence-bond order, in which one plane, for example, the xy-plane, is occupied by the  $|3x^2 - r^2\rangle$  orbital and the nearest neighbor ones is taken up with the  $|3y^2 - r^2\rangle$  orbital, etc. The degenerate ground state contains the alternating plaquette valence-bond component, in agreement with *Feiner et al.*'s result<sup>13</sup> by considering Gaussian quantum fluctuations. This also confirms the validity and the efficiency of our Cluster-SCF approach. In this case, the A-type AFM structure observed in realistic KCuF<sub>3</sub> is not the candidate of the ground state. On the other hand, the nearest-neighbor orbital correlation functions are significantly different from zero. The short-range orbital correlations are strong, indicating that the system with only the electronic SE interaction is a spin-orbital liquid phase.

In such a spin-orbital correlated system, the spin alignment strongly depends on the orbital configuration. In fact one could easily find that the system with the SE interaction is a spin-orbital liquid phase, rather than a spin-orbital ordered state. Due to the spin rotation symmetry, the spin interaction in the SE coupling is Heisenberg-like. After averaging over orbital freedom degree, the spin exchange coupling strength along the  $l$ -axis in Eq.(5) reads

$$J_s^l = \langle F(\vec{\tau}_i^l, \vec{\tau}_j^l) \rangle = J_1 + \frac{J_2}{2} (\langle I_i^l \rangle + \langle I_{j_l}^l \rangle) + J_3 \langle I_i^l I_{j_l}^l \rangle,$$

which is isotropic for the x-, the y- and the z-axes, such an interaction does not lead to the anisotropic A-type AFM structure in KCuF<sub>3</sub>, unless the orbital symmetry is broken. In the orbital part of the SE interaction in Eq.(2), after averaging over the spin coupling, the orbital part along the  $l$ -direction reads,

$$h_o^l = \frac{J_2}{2} \langle \vec{s}_i \cdot \vec{s}_{j_l} \rangle (I_i^l + I_{j_l}^l) + (J_3 \langle \vec{s}_i \cdot \vec{s}_{j_l} \rangle + J_4) I_i^l I_{j_l}^l, \quad (6)$$

The first term is similar to a magnetic field, called the orbital field. This orbital field is frustrated for the orbital occupation, which favors either  $|3z^2 - r^2\rangle$  or  $|x^2 - y^2\rangle$  orbitals along the  $z$ -axis; while along the  $x$  direction, it favors either  $|3x^2 - r^2\rangle$  or  $|y^2 - z^2\rangle$  orbitals. Unfortunately the orbital interaction part,  $I_i^l I_{j_l}^l$ , in Eq.(6) is also inherently frustrated: no matter what the coefficient of the second term in Eq.(6) is, negative or positive, this orbital correlation favors a frustrated ground state, as pointed by Khomskii et al.<sup>12</sup> On the one hand, if the coefficient of  $I_i^l I_{j_l}^l$  is negative, the orbital exchange coupling favors different ferro-orbital occupations along different directions, in accordance with the frustration of the orbital field mentioned above; on the other hand, if the coefficient is positive, the orbital polarizations in each bond arising from the orbital field are opposite to that arising from the orbital coupling, which enhances the frustration effect.

One notices that if the spin correlation functions are strongly anisotropic, the frustration effect is greatly suppressed. For example, as the spin correlation along the  $z$ -axis is so strong that  $\langle \vec{s}_i \cdot \vec{s}_{j_z} \rangle \approx -3/4$ , while the spin correlation functions along the  $x, y$ -axes almost vanish,  $\langle \vec{s}_i \cdot \vec{s}_{j_{x,y}} \rangle \approx 0$ , then the orbital part of the SE interaction becomes

$$h_o = J_4 \sum_i [I_i^x I_{i+x}^x + I_i^y I_{i+y}^y - 0.95 I_i^z I_{i+z}^z - 1.78 I_i^z] \quad (7)$$

the  $x, y$ -components of the orbital field approach to zero, leaving a large  $z$ -component in Eq.(7). Obviously the strong uniaxial orbital field suppresses the frustration of the orbital exchange coupling, and singles out the  $|3z^2 - r^2\rangle$  orbit in each site, forming the ferro-orbital order; our numerical calculation confirms this result. Also it could be shown that strongly anisotropic plaquette-valence-bond correlation of the spins favors the alternating plaquette-valence-bond orbital order. As we will shown later, the highly anisotropic magnetic correlation is the consequence of the orbital ordering in  $\text{KCuF}_3$ .

Neglecting the spin and orbital quantum fluctuations, Kugel and Khomskii<sup>3</sup> found the mean-field solution of the SE interaction is the A-type AFM and G-type/C-type AFO order. In fact, their classical approximation to the spins as the A-type AFM order introduced an orbital field ( $-\sum_i I_i^z$ ). This orbital field lifts most degenerate states of the orbital ground state, leaving the G-type and the C-type AFO configurations as the candidates; the fourfold rotation symmetry of the spin structure also confines the possible orbital ground state as the G-type or C-type AFO structure, in agreement with Goodenough-Kanamori empirical rule<sup>22</sup>. Nevertheless, the orbital field do not remove the degeneracy of the G-type and the C-type AFO structures, as shown in Ref.3. However, as found in the experiments<sup>11</sup>, the average magnetic moment of each Cu spin is about  $0.49 \mu_B$ , only a half of the classical expectation, suggesting that spin quantum fluctuations in  $\text{KCuF}_3$  is very strong, and the classical approximation to the spins is not appropriate.

The phonon-mediated orbital-orbital coupling with discrete cubic symmetry,  $H_{JT}$  in Eq.(3), is also strongly frustrated. It has the same impact on the orbital ground state as the second term in Eq.(6) does. Early treatment<sup>7</sup> to  $H_{JT}$  by the mean-field approach is questionable since the presumed orbital order was equivalent to introduce an artificial orbital field to break the orbital symmetry, however the orbital field did not really exist. We notice that  $H_{JT}$  can be absorbed in the second term in Eq.(6), so the combination of the JT orbital coupling  $H_{JT}$  and the SE interaction,  $H_{SE}$ , does not break the symmetry of spin and orbital in cubic crystal structure. Therefore in the absence of the crystalline field splitting from the static JT distortion, the ground state of the system is an orbital liquid or para-orbital phase. Accordingly, the orbital symmetry in  $\text{KCuF}_3$  should be broken by the static JT distortion, i.e. the orthorhombic CF splitting,  $H_{CF}$ . In what follows we explore the role of orthorhombic CF

splitting in the ground state in  $\text{KCuF}_3$ .

## B. Role of Orthorhombic Crystalline Field

In perovskite  $\text{KCuF}_3$  there exist two kind cooperative JT distortions at low temperature<sup>9,10</sup>. With respect to these two different small lattice distortions,  $\text{KCuF}_3$  exhibits two slightly different crystalline phases, the *type-d* and the *type-a* structures. The orbital ground state in the *type-a* structure differs from that in the *type-d* structure due to different orthorhombic CF splittings of the  $\text{CuF}_6$  octahedra.

We first study the orbital components of single Cu atom under the orthorhombic CF. For  $|V_x/V_z| = 2$ , the orbital wavefunctions always consist of two orbital patterns, a low energy pattern  $|a\rangle = 0.851|3z^2 - r^2\rangle \pm 0.526|3x^2 - y^2\rangle$ , in which the hole completely occupies this pattern at large  $|V_z|$ , and a high energy pattern  $|b\rangle = 0.526|x^2 - y^2\rangle \mp 0.851|3z^2 - r^2\rangle$ ; here ' $\pm$ ' refer to the two sublattices of the antiferro-distortion in the two crystalline phases. Approximately,  $|a\rangle \approx |y^2 - z^2\rangle$  and  $|b\rangle \approx |3x^2 - r^2\rangle$  for '+'; and  $|a\rangle \approx |x^2 - z^2\rangle$  and  $|b\rangle \approx |3y^2 - r^2\rangle$  for '-'. Such combinations are also consistent with the orthorhombic distortions of the  $\text{CuF}_6$  octahedra: if the Cu-F bond is elongated along the  $x$  axis, the CF singles out the  $|y^2 - z^2\rangle$  orbit, corresponding to '+'; on the other hand, if Cu-F bond is elongated along  $y$  direction, the energy of  $|x^2 - z^2\rangle$  orbit is lower, corresponding to '-'.

In the lattice case, the orthorhombic CF splitting competes with the SE interaction and the JT orbital coupling, the orbital occupation of Cu 3d holes depends not only on the CF splitting ratio  $|V_x/V_z|$ , but also on the magnitude of  $V_z$ . When  $|V_z|$  is very small, due to the orbital frustration and large quantum fluctuations, the orbital symmetry is not broken, and the ground state of the system is still an orbital liquid or para-orbital phase. The critical value of  $|V_z|$  breaking the orbital symmetry relies on the JT orbital coupling. For large  $|V_z|$ , the transverse CF splitting  $V_x$  alternating in the  $xy$ -plane in the *type-d* structure gives rise to C-type AFO configuration; as a contrast in the *type-a* structure, the staggered transverse CF splitting  $V_x$  in the  $x, y$  and  $z$  directions gives rise to G-type AFO configuration. At  $|V_z|=0.5J$ , the sublattice orbitalization and the orbital correlation functions listed in Table I definitely show the G-type AFO correlation in the *type-a* structure and the C-type AFO correlation in the *type-d* structure. Some magnetic properties in both structures are also collected in Table I. Therefore the presence of the orthorhombic CF breaks the discrete orbital symmetry, suppresses the orbital frustration and quantum fluctuation, and establishes the long-range orbital order in  $\text{KCuF}_3$ .

As soon as the orthorhombic CF singles out the orbital structure, it also stabilizes the magnetic structure simultaneously, hence the spin-orbital ground state. Under the full Hamiltonian, our numerical results show that

the magnetic ground states are the A-type AFM order both for the *type-a* and for the *type-d* crystalline phases. And the spin correlations are strongly anisotropic,  $\langle \vec{s}_i \cdot \vec{s}_{j_z} \rangle / \langle \vec{s}_i \cdot \vec{s}_{j_{x,y}} \rangle \approx 10$ . Furthermore, we obtain the spin coupling strengths  $J_z$  and  $J_{x,y}$ , which are 16.6 meV and 0.64 meV, respectively, giving rise to  $|J_z/J_{x,y}|$  about 26 for  $V_z = -0.5J$ , as shown in Fig.1. These results are in

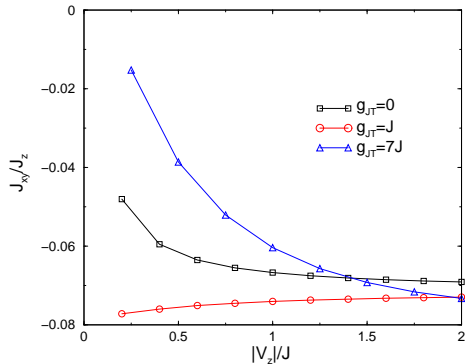


FIG. 1: Dependence of the ratio of N.N spin coupling strengths  $J_{x,y}/J_z$  on orthorhombic CF splitting  $|V_z|/J$ . Here  $J$  is the energy scale of the SE coupling.

agreement with the experimental data in  $\text{KCuF}_3^{1,2,11}$ . Such strong anisotropy in spin correlations and magnetic couplings is attributed to the anisotropic regular distribution of the orbital wavefunctions in real space, i.e., the orbital ordering, as we will show later.

Next we focus on the magnetic moment of each Cu spin. We find that the effective magnetic moment of each Cu spin is considerably reduced from  $1 \mu_B$  to  $0.496 \mu_B$ , the averaged spin of each Cu ion decreases to 0.248, about a half of  $1/2$ , consistent with the neutron scattering experimental data very well<sup>11</sup>. The theoretical and experimental results are listed in Table I. Obviously such great reduction of the magnetic moment arises from the spin-orbital quantum fluctuations: one possibility is from the low-dimensional AFM spin-wave excitation; the another is from the spin-and-orbital wave excitation in the spin-orbital system<sup>14</sup>, which causes more spin flipping via the spin-orbital interaction. From Table I, one finds the discrepancy between the present ratio of  $|J_z/J_{x,y}|$  ( $\approx 26$ ) and Satija's experimental fitting data ( $|J_z/J_{x,y}| \approx 100$ )<sup>23</sup>, we attribute this discrepancy to the frozen of the orbital excitations in his fitting to the experimental data. According to the spin exchange couplings shown in Table I, we find that in the mean-field approximation, the theoretical *Neel* temperature of  $\text{KCuF}_3$  is about, 37 K, in agreement with the experimental data 39 K in *type-a* structure, confirming that our choice to the theoretical parameters  $t$ ,  $U$ ,  $J_H$ ,  $g_{JT}$  and  $V_z$  is appropriate.

In fact the influence of the orthorhombic CF splitting and the JT orbital coupling on the magnetic moment is not monotonously. As shown in Fig.2, the phonon-mediated JT orbital coupling and the orthorhombic CF distortion play distinct roles in the magnetic moments through affecting the orbital quantum fluctuations and

TABLE I: Calculated and experimental averaged spin, magnetic couplings, nearest-neighbor spin correlations, orbitalization and orbital correlations. 'a' and 'd' refer *type-a* and *type-d* phases.  $J_{x,y,z}$  are in units of  $meV$ . The theoretical parameters are  $g_{JT} = 7J$ , and  $|V_z| = 0.5J$ .

|                    | $\langle s \rangle$      | $\langle J_{x,y} \rangle$ | $\langle J_z \rangle$                                   | $\langle \vec{s}_i \cdot \vec{s}_j \rangle_{x,y}$   | $\langle \vec{s}_i \cdot \vec{s}_j \rangle_z$ |
|--------------------|--------------------------|---------------------------|---|---|---|
| Calc.              | 0.248                    | -0.64                     | 16.6  | 0.070   | -0.684  |
| Expt.              | $0.245^{11}$             | $-0.2^{23}$               | $17.5^{23}$   |   |   |
|                    | $\langle \tau_z \rangle$ | $\langle \tau_x \rangle$  | $\langle \vec{\tau}_i \cdot \vec{\tau}_j \rangle_{x,y}$ | $\langle \vec{\tau}_i \cdot \vec{\tau}_j \rangle_z$ |   |
| Calc. <sup>d</sup> | 0.077                    | 0.492                     | -0.251  | 0.249   |   |
| Calc. <sup>a</sup> | 0.077                    | 0.492                     | -0.251  | -0.280  |   |

the orbital ordering. At small splitting  $|V_z|$  and in the absence of the JT coupling,  $g_{JT} = 0$ , the orbital field  $-I_i^z$  in the A-type AFM structure is much stronger than that from the CF splitting, resulting in large orbital polarization with dominant  $|3z^2 - r^2\rangle$  orbit; with the increase of the CF splitting, the transverse CF term  $V_x$  mixes the  $|3z^2 - r^2\rangle$  orbit with the  $|x^2 - y^2\rangle$  orbit, leading to the descent of the sublattice orbitalization, as seen in Fig.2a. Meanwhile the decrease of the orbitalization weakens the low-dimensionality of the spin correlations, the magnetic moment gradually lifts with increasing CF splitting, which can be seen in Fig.2b. At sufficient large  $|V_z|$ , the orbital occupation is full polarized at the  $|a\rangle$  orbit, and the magnetic moment saturates to  $0.61 \mu_B$  per site. In this situation, a small CF splitting favoring of the A-type AFM structure produces strong local orbital field and orbital polarization, suppresses the orbital frustration from the superexchange coupling. With the further increase of the CF splitting, the transverse component of the CF splitting  $V_x$  mixes the orbitals  $|3z^2 - r^2\rangle$  and  $|x^2 - y^2\rangle$ , the orbital polarization declines and the anisotropy of orbital and spin correlations become weak, hence the ratio of the magnetic couplings  $J_z/J_{x,y}$  decrease with the increase for very large CF splitting, as seen in Fig.1.

When the JT orbital coupling is taken into account, the dependences of the spin coupling, the sublattice orbitalization and the magnetic moment on  $|V_z|$  are different for  $g_{JT}/J=1$  and for  $g_{JT}/J=7$ . The different behaviors arise from the distinct effects of the CF splitting on the local orbital field and the frustration term. At  $g_{JT}/J=1$ ,  $|J_x/J_z|$  is larger than that at  $g_{JT}=0$ , implying the low-dimensional characters of the spin correlations and the spin fluctuations become weak. This leads to large magnetic moment and small anisotropy, as we find in Fig.1 and Fig.2b. The weakness of the anisotropy of the magnetic couplings at  $g_{JT}/J=1$  arises from the frustration enhancement comparison with that at  $g_{JT}=0$ . Our numerical results show that at  $g_{JT}/J=1$ , the further increase in the CF splitting is almost balanced by the orbital field and the frustrated orbital-orbital couplings, hence the spin and the orbital correlations, the sublattice orbital-

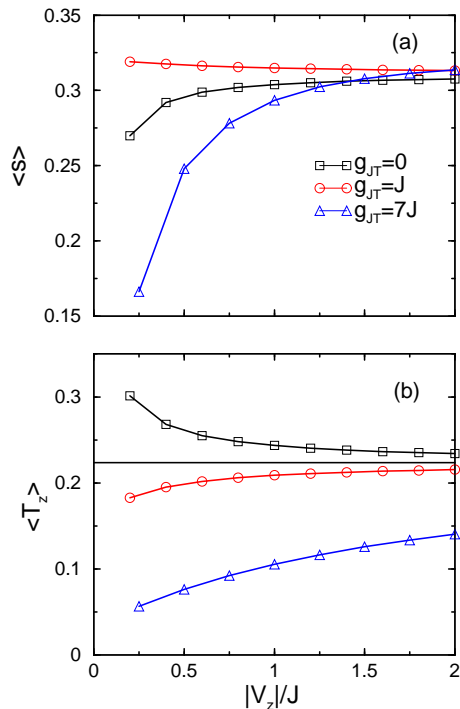


FIG. 2: Dependence of averaged spin (a) and sublattice orbitalization (b) on orthorhombic CF splitting in different JT orbital coupling.

ization and sublattice magnetization and the magnetic coupling almost do not change with the increase of the CF splitting, as shown in Fig.1 and Fig.2.

In contrast, the large JT orbital coupling at  $g_{JT} = 7J$  leads to strong orbital fluctuation, hence to small sublattice orbitalization and magnetization in Fig.2. In this situation, one would expect more weak anisotropy or large ratio  $|J_x/J_z|$ ; however as shown in Fig.1, one curiously finds that the anisotropy is the most strong, in comparison with  $g_{JT} = 0$  and  $g_{JT} = J$ . We find this strong anisotropy may come accidentally in small orthorhombic CF splitting: in the spin coupling along the  $x$ -axis, the sign of the constant part  $J_1$  is contrary to that from the other terms, which leads to  $J_x$  be very small, hence small ratio  $|J_x/J_z|$  and large anisotropy. Strong orbital fluctuations also excite spin flipping excitation via the spin-orbital coupling. Thus the magnetic moment critically decreases to  $0.49 \mu_B$  at  $|V_z|/J = 0.5$ . Further increase of the orthorhombic CF splitting greatly suppresses the orbital and spin fluctuations, and the sublattice magnetic moment and the orbitalization rise a lot. With the further increase of the orthorhombic CF splitting, the anisotropy becomes more weak, and the sublattice magnetization  $\langle S \rangle$  and orbitalization  $\langle T_z \rangle$  further increase gradually.

#### IV. RESONANT X-RAY SCATTERING FOR ORBITAL ORDER

The orbital ordering in  $\text{KCuF}_3$  can be manifested in the RXS peaks utilizing the sensitivity of x-ray scattering to the anisotropic density of orbital ordered electrons<sup>1,2</sup>. The anisotropy of spatial electronic clouds gives rise to the anomalous tensor component in atomic scattering factor, and the interference of these atomic scattering amplitudes in the presence of long-range orbital order leads to the orbital superlattice reflection at the structural forbidden position. Obviously, it is more directly to identify the orbital ordering using the spectral line shapes of the quadrupole  $1s - 3d$  scattering, contrary to the complicated spectra of the  $1s - 4p$  dipole scattering which is often used in present experiments<sup>1,2</sup>, although the signal enhancement of the quadrupole scattering is weaker than the dipole scattering<sup>24,25,26</sup>. In the following we present the azimuthal angle dependence of the  $1s - 3d$  RXS intensity to directly demonstrate the character of the orbital order in  $\text{KCuF}_3$ .

For the C-type AFO ordered ground state with *type-d* structure, the orbital ordering peaks reflect at  $(h, k, l) = (\text{odd}, \text{odd}, \text{even})$ , which are forbidden for the structural and magnetic reflections. The sublattice orbital wavefunctions consist of two different components:  $|\psi_1\rangle = \alpha_1|3z^2 - r^2\rangle + \alpha_2|x^2 - y^2\rangle$  and  $|\psi_2\rangle = \alpha_1|3z^2 - r^2\rangle - \alpha_2|x^2 - y^2\rangle$ , here the coefficients  $\alpha_{1,2}$  are the functions of the interaction parameters. Then the orbital structural factor is read as:

$$F_{hkl} = f(\Gamma, r_{2,ds}, c, \omega) \sqrt{n_{\epsilon k} n_{\epsilon' k'}} \alpha_1 \alpha_2 \{ \epsilon_z k_z (\epsilon'_x k'_x - \epsilon'_y k'_y) + (\epsilon_x k_x - \epsilon_y k_y) \epsilon'_z k'_z \} \quad (8)$$

where the function  $f(\Gamma, r_{2,ds}, c, \omega)$  is the coefficient depending on the lifetime of the intermediate states,  $\Gamma$ , the radial matrix element  $r_{2,ds}$ , the velocity of photon  $c$  and the incoming photon frequency  $\omega$ ;  $n_{\epsilon(\epsilon'), k(k')}$  is the density of the incoming (outgoing) beam of photons with polarization  $\vec{\epsilon}(\vec{\epsilon}')$  and wavevector  $\vec{k}(\vec{k}')$ . The azimuthal angle dependence of the RXS intensity is shown in Fig.3 at  $(1, 1, 0)$  reflection for unrotated ( $\sigma\sigma'$ ) and rotated ( $\sigma\pi'$ ) channels for the perfect  $\sigma$  polarized incoming beam. As a comparison, we also present the azimuthal angle dependence of the RXS intensity in Fig.4 for the G-type AFO order with *type-a* structure at  $(3, 3, 1)$  reflection.

Due to the difference of the orbital superlattice for the C-type and the G-type AFO orders, the RXS peaks appear at different orbital reflections with  $(\text{odd}, \text{odd}, \text{even})$  for the C-type orbital order in the *type-d* structure, and with  $(\text{odd}, \text{odd}, \text{odd})$  for the G-type orbital order in the *type-a* structure. These sublattice reflections distinguish these orbital orders in different crystalline phases of  $\text{KCuF}_3$ . The azimuthal angle dependence of the RXS intensities exhibits different periods in the *type-d* and the *type-a* structures, as seen in Fig.3 and Fig.4. The periods are  $\pi$  and  $2\pi$  for the  $\sigma - \pi'$  channel in these two structures, respectively; and are  $\pi/2$  and  $\pi$  for the  $\sigma - \sigma'$  channel

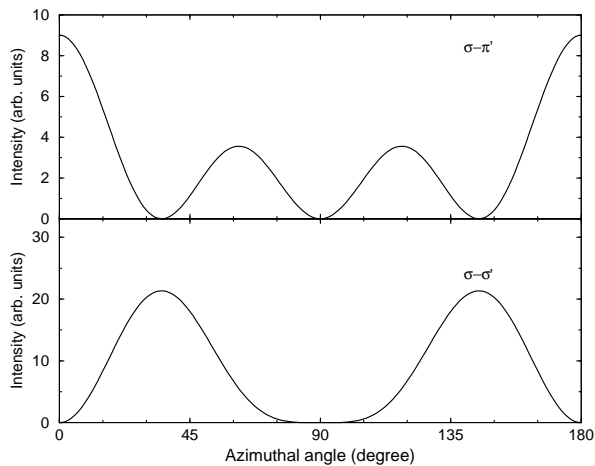


FIG. 3: The azimuthal angle dependence of the orbital (1,1,0) reflection intensity for unrotated ( $\sigma\sigma'$ ) and rotated ( $\sigma\pi'$ ) channels in C-type AFO.

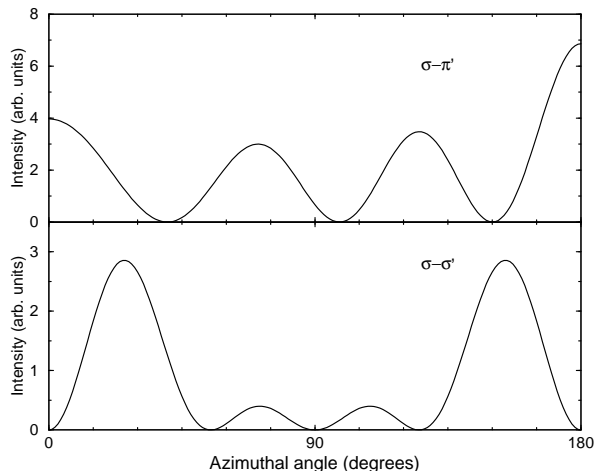


FIG. 4: Azimuthal angle dependence of the orbital (3,3,1) reflection intensity for unrotated ( $\sigma\sigma'$ ) and rotated ( $\sigma\pi'$ ) channels in G-type AFO.

respectively. Distinct line shapes of the RXS scattering intensities in the  $\sigma-\sigma'$  channel also easily identify the two orbital AFO orders. The different periods are attributed to the different orbital structures along the  $z$ -axis. One may expect that the  $4p$  orbitals of Cu hybridizing with  $3d$  orbitals will modify the present  $1s-3d$  scattering line shape, but not the period.

## V. REMARKS AND SUMMARY

We notice that in perovskite  $\text{KCuF}_3$ , the nonresonant magnetic scattering experiment<sup>1</sup> showed that the orbital angular momentum  $L$  contribute finite value the total magnetic moment, and  $L/S \approx 0.29$ . Obviously the finite orbital moment does not come from the two  $e_g$  orbitals,

since the expectation of the orbital angular momentum  $L$  in the orbital basis wavefunctions  $|3z^2 - r^2\rangle/|x^2 - y^2\rangle$  and any of their combinations is zero. One possibility of such considerable residual orbital moment is attributed to the reduced symmetry of the  $t_{2g}$  orbitals in  $\text{KCuF}_3$ <sup>27</sup> or a small fraction of the  $t_{2g}$  orbit mixing with the  $e_g$  orbit; another possibility is from the hybridization of the  $4p$  orbitals with the  $e_g$  orbitals. In both situations the weak  $LS$  coupling in  $\text{KCuF}_3$  will not change the spin alignment considerably.

In the numerous literatures on  $\text{KCuF}_3$ , some authors<sup>5,13,14</sup> took the tetragonal CF splitting into account to stabilize the A-type AFM order, but the degeneracy of the G-type and the C-type AFO orders is not lifted, so the ground state under the tetragonal CF is still indefinite. Only in the present theory the full consideration of the orthorhombic CF splitting,  $V_z$  and  $V_x$ , together with the JT orbital coupling and the SE coupling, can we determine the ground state exclusively, and consistently interpret the experimental data. Furthermore, considering many other spin-orbital-lattice interacting compounds, such as manganites<sup>28,29,30</sup>, vanadium oxides<sup>20,31</sup>, and titanium oxides<sup>32,33,34,35</sup>, in which the CF splitting arising from the lattice distortion extensively exists, one may find such a fact that the low-symmetric CF splittings play crucial roles in singling out many degenerate candidates as the sole orbital ordered ground state. Thus a conclusion arrives that *the highly degenerate ground state in the correlated electronic system with pure spin-orbital interactions usually stabilizes through distorting to a lower symmetry phase*, which is a natural generalization of the Jahn-Teller effect in strongly correlated systems. Detail results will be presented in further study.

In summary, we have performed a systematic study on the roles of the electronic SE interaction, the JT orbital coupling and the orthorhombic CF splitting in the orbital ordering and the magnetic properties in  $\text{KCuF}_3$ . The SE and effective JT orbital coupling lead to a orbital liquid state due to the inherent frustration and orbital quantum fluctuations. The orthorhombic CF lowers the orbital symmetry, and stabilizes the orbital ordering as the observed in experiment. The orbital ordering results in the strong magnetic anisotropy. Strong spin fluctuation and the orbital frustration considerably reduce magnetic moment of Cu spins.

## Acknowledgments

Authors thanks N. Binggeli for providing the electronic structure data of  $\text{KCuF}_3$ . Great appreciate is devoted to G. Sandro, M. Fabrizio and M. Altarelli in developing the Cluster-SCF method. Supports from the NSF of China and the BaiRen project from the Chinese Academy of Sciences (CAS) are appreciated. Part of numerical calculation was performed in CCS, HFCAS.

- 
- <sup>1</sup> R. Caciuffo, L. Paolasini, A. Sollier, P. Ghigna, E. Pavarini, J. Van de Brink, and M. Altarelli, *Phys. Rev. B* **65**, 174425 (2002).
- <sup>2</sup> L. Paolasini, R. Caciuffo, A. Sollier, P. Ghigna, and M. Altarelli, *Phys. Rev. Lett.* **88**, 106403 (2002).
- <sup>3</sup> K. I. Kugel and D. I. Khomskii, *Sov. Phys. JETP* **37**, 725 (1973).
- <sup>4</sup> A. I. Liechtenstein, V. I. Anisimov and J. Zaanen, *Phys. Rev. B* **52**, R5467 (1995).
- <sup>5</sup> J. E. Medvedeva, M. A. Korotin, V.I. Anisimov, and A. J. Freeman, *Phys. Rev. B* **65**, 172413 (2002).
- <sup>6</sup> J. Kanamori, *J. Appl. Phys.* **31**, 14S. (1960).
- <sup>7</sup> B. Halperin and R. Engelman, *Phys. Rev. B* **3**, 1698 (1971).
- <sup>8</sup> M. Kataoka, *J. Phys. Soc. Japan* **70**, 2353 (2001).
- <sup>9</sup> A. Okazaki and Y. Suemune, *J. Phys. Soc. Japan* **16**, 176 (1961).
- <sup>10</sup> R. H. Buttner, E. N. Maslen and N. Spadaccini, *Acta Cryst. B* **46**, 131 (1990) (2001).
- <sup>11</sup> M. T. Hutchings, E. J. Samuelsen, G. Shirane, and K. Yamada, *Phys. Rev.* **188**, 919 (1969).
- <sup>12</sup> D. I. Khomskii and M. V. Mostovoy, *J. Phys. A: Math. Gen.* **36**, 9197 (2003).
- <sup>13</sup> L. F. Feiner, A. M. Oles, and J. Zaanen, *Phys. Rev. Lett.* **78**, 2799 (1997).
- <sup>14</sup> A. M. Oles, L. F. Feiner, and J. Zaanen, *Phys. Rev. B* **61**, 6257 (2000).
- <sup>15</sup> G. Khaliullin, and V. Oudovenko, *Phys. Rev. B* **56**, R14243 (1997).
- <sup>16</sup> L. F. Feiner, A. M. Oles, and J. Zaanen, *J. Phys.: Condens. Matter*, **10**, L555 (1998); M. Imada, A. Fujimori, and Y. Tokura, *Rev. Mod. Phys.* **70**, 1039 (1998).
- <sup>17</sup> N. Binggeli, and M. Altarelli, *Phys. Rev. B* **70**, 085517 (2004).
- <sup>18</sup> C. Castellani, C. R. Natoli, and J. Ranninger, *Phys. Rev. B* **18**, 4945 (1978).
- <sup>19</sup> K. I. Kugel and D. I. Khomskii, *Sov. Phys. Usp.* **25**, 231 (1982).
- <sup>20</sup> Liang-Jian Zou, M. Fabrizio and M. Altarelli, *Preprint*.
- <sup>21</sup> Dong-Meng Chen and Liang-Jian Zou, *cond-mat/0501155* (2005).
- <sup>22</sup> J. B. Goodenough, *Magnetism and Chemical Bond* (Interscience, New York, 1963)
- <sup>23</sup> S. K. Satija, J. D. Axe, G. Shirane, H. Yoshizawa, and K. Hirakawa, *Phys. Rev. B* **21**, 2001 (1980).
- <sup>24</sup> Y. Murakami, H. Kawada, H. Kawata, M. Tanaka, T. Arima, Y. Moritomo and Y. Tokura, *Phys. Rev. Lett.* **80**, 1932 (1998).
- <sup>25</sup> M. Fabrizio, M. Altarelli and M. Benfatlo, *Phys. Rev. Lett.* **80**, 3400 (1998); *Phys. Rev. Lett.* **81**, E4030 (1998).
- <sup>26</sup> S. W. Lovesey, K. S. Knight and E. Balcar, *Phys. Rev. B* **64**, 054405 (2001).
- <sup>27</sup> M. Hidaka, T. Eguchi, and I. Yamada, *J. Phys. Soc. Jpn.* **67**, 2488 (1998).
- <sup>28</sup> R. Shiina, T. Nishitani, and H. Shiba, *J. Phys. Soc. Jpn.* **66**, 3159 (1997).
- <sup>29</sup> T. Mizokawa, D. I. Khomskii, and G. A. Sawatzky, *Phys. Rev. B* **60**, 7309 (1999)
- <sup>30</sup> R. Y. Gu and C. S. Ting, *Phys. Rev. B* **65**, 214426 (2002).
- <sup>31</sup> A. Tanaka, *J. Phys. Soc. Jpn.* **71**, 1091 (2002).
- <sup>32</sup> M. Cwik, T. Lorenz, J. Baier, R. Muller, G. Andre, F. Bouree, F. Lichtenberg, A. Freimuth, R. Schmitz, E. Muller-Hartmann, and M. Braden, *Phys. Rev. B* **68**, 060401 (2003).
- <sup>33</sup> R. Schmitz, O. Entin-Wohlman, A. Ahaony, A. B. Harris, and E. Muller-Hartmann, *cond-mat/0407524* (2004).
- <sup>34</sup> M. W. Haverkort *et al.*, *Phys. Rev. Lett.* **94**, 056401 (2005).
- <sup>35</sup> S. V. Streltsov, A. S. Mylnikova, A. O. Shorikov, Z. V. Pchelkina, D. I. Khomskii, and V. I. Anisimov, *cond-mat/0504281* (2005).